Varved sediment responses to early Holocene climate and environmental changes in Lake Meerfelder Maar (Germany) obtained from multivariate analyses of µ-XRF core scanning data

Celia Martin-Puertas[1,2*], Rik Tjallingii[1*], Menno Bloemsma[3,4], and Achim Brauer[1]

[1] GFZ-German Research Centre for Geosciences, Section 5.2 Climate Dynamics and Landscape Evolution, Telegrafenberg, Potsdam D-14473, Germany.

[2] Department of Geography, Royal Holloway, University of London, Egham, Surrey TW20 0EX, United Kingdom.

[3] Delft University of Technology, Faculty of Civil Engineering and Geosciences, Department of Geotechnology, Stevinweg 1, NL-2628CN Delft, The Netherlands

[4] Tata Steel - Netherlands Main Office, Postbus 10000, 1970 CA IJmuiden, The Netherlands

e-mail: celia.martinpuertas@rhul.ac.uk, rik.tjallingii@gfz-potsdam.de

Abstract

We present an early-Holocene record from Lake Meerfelder Maar in Germany for in-depth interpretation of depositional changes in annually-laminated lake sediments as proxies for climatic and local environmental changes. We characterised the compositional changes in the sediment record using Ward's clustering analyses of the µ-XRF core scanning data and linked these to microfacies description. Down-core distribution of the clusters allowed defining boundaries that represent variations of a comprehensive element assemblage occurring at 11 555, 11 230, 10 650, 10 515 and 9670 varve a BP. Our main results show that during the early Holocene the long-term vegetation reorganisation and evolution of the lake's catchment played a predominant role for sediment deposition. Abrupt shifts occurred at the Younger Dryas/Holocene and the Preboreal/Boreal biostratigraphical boundaries. We do not observe clear signals corresponding to known short-term climatic oscillations described in the North Atlantic region like the Preboreal Oscillation. A unique and intriguing episode in the history of the lake of predominantly organic deposition and very low amounts of allochthonous sediments occurred between 10 515 and 9670 varve a BP and is related to hydrological thresholds.

Keywords: varved lake sediments, clustering of µ-XRF core scanning data, early Holocene, central Europe.

1. Introduction

Annually-laminated (varved) lake sediments provide continuous information of climate change and landscape evolution in the human habitat. These sediment records allow the study of both long-term and abrupt climatic changes with seasonal time resolution before the instrumental period (Brauer et al., 1999; Martin-Puertas et al., 2012; Czymzik et al., 2013). The most recent techniques for the study of varved records include parallel investigation of microfacies analyses and geochemical information derived from micro X-ray fluorescence (µ-XRF) core scanning data (Dulski et al., 2015). This approach improves the interpretation of the observed chemical signals because those can be directly compared to observations of microfacies changes, which provide a better description of the sediments. However, characterization of sedimentological changes using single elements might give a simplistic interpretation of the climatic and environmental processes, as these changes are often related to variations in element assemblages (Bloemsma et al., 2012). So, studying variability of element assemblages rather than single elements can provide a better understanding of lake sedimentation and particularly on mechanisms of varve formation. By adopting this novel approach it will be possible to objectively distinguish even more subtle geochemical changes in the sediment record that would remain undetected by conventional analyses, as well as to establish if the control on sedimentation patterns is driven by land cover changes induced by natural vegetation succession or short-lived climatic events.

During the transition into the present interglacial conditions between 11 590 and 9000 years before present (a BP), the climatic and environmental conditions in central Europe were characterised by large climatic re-organisations that were regionally differently influenced by the progressive melting of the Fennoscandian ice sheet and rising sea level including flooding of the North Sea basin (Björck 2008). Northern Hemisphere air temperature variability reconstructed from $\delta^{18}O$ isotope records in Greenland (Masson-Delmotte et al., 2005; Rasmussen et al., 2014) and in central Europe (Grafenstein et al., 1999) show an initial abrupt warming followed by a further gradual temperature increase. This resulted in a rapid shift from the cold continental conditions of the Younger Dryas (YD) to temperate climate with milder winters and warmer summers in central Europe (Renssen, 2001). Short-lived synchronous $\delta^{18}O$ anomalies in the Greenland ice cores are superimposed on this multi-centennial timescales trend at 11.4, 10.3 and 9.3 thousand years before AD 2000 (ka b2k) (Rasmussen et al., 2014). These rapid isotope excursions have been related to cool pulses in the North Atlantic realm, *i.e.* the so-called ‘Preboreal Oscillation’ (PBO), ‘Boreal Oscillation’ (BO) and the ‘9.3 ka event’, respectively (e.g. Björck et al., 1997; McDermott et al., 2001; Wohlfarth et al., 2007; Bos et al., 2007; Lauterbach et al., 2011).

In northern and central Europe, the most significant environmental responses at the transition to interglacial conditions were the re-forestation through a plant succession influenced not only by climate but also by re-immigration of species from their glacial refugia in southern Europe and soil formation. The initial phase of the Holocene was still dominated by *Betula* and *Pinus* (Preboreal period in the Blytt-Sernander classification) and followed by an expansion of *Corylus* (Boreal period) (Litt et al., 2009; Theuerkauf et al., 2014). In northern-central Europe, short-term interruptions of forest development have been reported to coincide with the rapid cold oscillations, especially the ‘PBO’ (Björck et al., 1997; Bos et al., 2007).

The pollen record from the varved sediments of Lake Meerfelder Maar (MFM, Germany) captures the vegetation succession described in central Europe throughout the early Holocene at 20-100 year resolution (Litt et al., 2009) but does not record the short-term fluctuations. These pollen data can be directly compared to our seasonally resolved sediment proxies from MFM, giving the opportunity to study differences and similarities between the vegetation- and the lake response to shifting environmental and climatic conditions. Previous studies on the MFM sediments link changes in varve thickness and composition to large-scale climatic changes such as the onset and termination of the YD (Brauer et al., 1999), but also lower amplitude fluctuations during the late Holocene like the `2.8 ka oscillation´ (Martin-Puertas et al., 2012a). During the early Holocene, the climatic signal in the MFM sediments is, however, still in discussion (Martin-Puertas et al., 2012b).

In this paper we want to test advanced clustering for the total µ-XRF core scanning dataset as a suitable tool to better depict environmental and climatic changes in the geochemical record. Our specific objective is to investigate to what extend changes in sediment deposition respond to either the long-term changes of the surface conditions in the catchment and/or short-term climatic oscillations.

2. Study site

Lake Meerfelder Maar is located in the Westeifel Volcanic Field, Germany (50° 06’N, 6° 45’E). The lake is within a steep-sided volcanic crater, where the crater walls have a relief of 170 m. The lake is located at 336.5 m a.s.l., and has a water depth of up to 18 m. The modern lake surface area is 0.248 km^2, covering the northern part (ca 1/3) of the maar crater area (Fig. 1). The southern part is formed by a shallow delta plain, deposited during the last glacial period by the Meerbach stream that entered the crater from the south (Brauer et al., 1999). In historical times, the course of this stream has been changed several times for water regulation purposes. Today, it passes the crater south of the lake and exits the crater through a narrow gorge in the southeast (Fig. 1). The modern catchment is formed only of the crater (1.52 km^2) but the catchment has been almost four times larger (5.76 km2) in the past, when the Meerbach stream still discharged into the lake. The course of this stream has a great influence on the water balance and the sediment supply to the lake (Negendank et al., 1990). Due to the morphology of the crater, a rise in lake level of only 2 or 3 m would result in a three times larger lake surface, by flooding most of the southern delta plain and creating a large shallow water area (Brauer et al., 1999). Past lake level changes have been identified by former lake terraces, which, however, are of unknown age (Negendank et al., 1990). Due to its particular morphological situation in a deep maar crater (Fig. 1), MFM is wind-sheltered favouring the preservation of fine seasonal layers within the sediment sequence. There is only a hiatus of ca 240 varve years, which was recognized by microscopic investigation at ca 9700 varve a BP (Brauer et al., 2000).

The temperate climate of the region is influenced by the Atlantic Ocean.

Present day temperature varies from -0.3 °C (mean winter air temperature) to 16.3 °C (mean summer air temperature). Mean annual precipitation is of 950 mm, which reaches the highest monthly values in winter (Litt et al., 2009).

[INSERT FIGURE 1 HERE]

3. Material and Methods

In this study we use sediment cores collected during two coring campaigns in 1996 (MFM-6) and 2009 (MFM-09). The MFM-6 cores have been obtained with a Usinger piston-coring device (Brauer et al., 1999), while the MFM09 cores were recovered using a UWITEC piston corer (Martin-Puertas et al., 2012b). The 11.20 m long MFM-6 composite profile was composed of five individual core sequences (Brauer et al., 2000), while the 11.71 m long MFM09 composite profile was made combining two core sequences (MFM09-A and MFM09-D). All cores from both MFM-6 and MFM09 composite profiles were correlated using macro- and microscopic layers (Table 1, Fig. 2).

Varve counting and detailed thickness measurements for each individual varve were carried out on thin sections (120 x 35 mm), with a 2 cm overlap, using a petrographic microscope under plane and cross polarized light (100 x magnification) (Brauer et al., 1999).

[INSERT TABLE 1 HERE]

3.1 μ-XRF core scanning and multivariate analyses

We used the cores recovered in 2009 to analyse the chemical sediment composition of MFM. Measurements were carried out at 0.2 mm resolution with the ITRAX μ-XRF-core scanner at GFZ-Potsdam, Germany (Martin-

Puertas et al., 2012b). The high-resolution measurements provide 1–16 geochemical data points per varve depending on the annual sedimentation rate (varve thickness). The µ-XRF core scanner irradiated the split core surface with a Mo X-ray source for 20 s, operated at 30 kV and 40 mA, generating energy dispersive XRF radiation. This way, the element intensities of Si, K, Ca, Ti, Mn, Fe, Ni, Rb, Sr and Zr as well as relative variations of the coherent and incoherent radiation were acquired non-destructively. The measured chemical composition of the sediment is expressed as element intensities (cps), which are non-linearly correlated to element concentration due to changing matrix effects, physical properties, and geometry of the sample throughout the core (e.g. Tjallingii et al. 2007). The easiest and most convenient way to eliminate such specimen effects is by using log-ratios of two elements, which are linear functions of log-ratios of element concentrations (Weltje and Tjallingii, 2008). Additionally, the log-ratio transformation of element intensities resolves many difficulties associated with closed-sum data that inhibit rigorous multivariate statistical analyses. The precise correlation between the composite profiles MFM-6 and MFM09 based on well-defined marker layers (Martin-Puertas et al., 2012b) allowed transferring the µ-XRF data on to the age scale though the age depth model performed for the sedimentary profile (Table 1, Fig. 2).

Statistically robust clustering analysis allows for objective compositional classification with out prior knowledge. The Ward's hierarchical clustering analysis was applied on the complete set of XRF measurements of MFM-09 (n = 5635) after centered log-ratio (*clr*) transformation (e.g. Aitchison, 1982) of the µ-XRF scanning data following:

$$clr\ I_{ij} = ln(I_{ij}/gm_j) \qquad (1)$$

Here, I_{ij} is the element intensity of element *i* in measurement *j* and gm_j is the geometric mean of all elements analysed at measurement *j*. Hierarchical clustering results are typically presented by a dendrogram with the number clusters vs. the Euclidian linking-distances between the clusters. As the number of clusters increase, the linking distances decreases, due to a reduction of the statistical differences. The objective of the Ward's hierarchical clustering analysis is to obtain a minimum number of clusters that provides a satisfactory description of the studied sediments. More details on the compositional differences of the individual clusters were obtained from biplots, which visualise the loadings (variables) of the principal component analyses (PCA).

4. Results

4.1. Chronology

The MFM sediments are varved for most of the Holocene and Lateglacial. A floating varve chronology extending from ca. 1500 back to 14 200 cal a BP was established and anchored to an ‘absolute’ time scale using the Ulmener Maar Tephra (UMT) isochrones dated at 11 000 ± 110 cal a BP in Lake Holzmaar sediments (Zolitschka et al., 2000) as isochrone (Brauer et al., 2000). This chronology is supported by 43 ^{14}C dates on terrestrial plant macrofossil remains and published as `MFM-2000 chronology´ (Brauer et al., 2000). Varve interpolation was applied where varves are not preserved (dashed line in Fig. 2). Major interpolated interval occurs at the YD/Holocene boundary, where 52 varves were interpolated along 6 cm of poor varve preservation between 11 640 and 11 590 varve a BP (marker layer YD, Table 1), and at 9670 varve a BP (40 varves below marker layer K644, Table 1) 240 years were included in the chronology to fill the gap of a hiatus (see details in Brauer et al. 2000). The MFM-2000 has been updated and published as `MFM-2012 chronology´ (Martin-Puertas et al., 2012b). Re- counting on the new MFM09 composite profile was carried out for the interval between maker layers KL7-KL1 (7796-2058 varve a BP). Comparison between the MFM2012 and MFM2000 chronologies along this interval (5738 varves) reveals counting deviations of less than 0.5% (29 varves), thus confirming the MFM2000 count. In this paper, we use the MFM2000 chronology for the study interval (11 640 - 9000 varve a BP), which has been transferred in the MFM09 composite profile using macro- and microscopic marker layers (Table 1, Fig. 2).

[INSERT FIGURE 2 HERE]

4.2. Microfacies analyses

The early Holocene sediments of MFM have been broadly identified as organic-diatomaceous varves with varying amount of detrital matter and irregularly intercalated distinct graded detrital layers (Fig. 3). Two different organic varve facies are distinguished. Organic varve facies 1 represents varves formed by couplets of spring / summer sub-layers made up of one or two different monospecific planktonic diatom blooms of *Stephanodiscus sp.* and/or *Cyclotella sp*., and autumn / winter sub-layers composed of organic detritus, reworked littoral diatoms and detrital silt and clays (Fig. 3b, c). Varve thickness varies between 0.24 to 3.2 mm. Organic varve facies 2 shows thinner varves (0.2 mm) formed by triplets of diatom bloom, endogenic calcite and amorphous and particulate organic detritus sub-layers, where the minerogenic content is low (Fig. 3b, c). Additionally, early diagenetic (vivianite, pyrite) and synsedimentary (siderite) iron-rich minerals are common throughout the cores, commonly dispersed within the sediments (Brauer et al., 2000; Martín-Puertas et al., 2012b).

The later half of the YD (below 756 cm) is characterised by a different varve facies, i.e. clastic-organic varves with graded silt layer at the base of each varve (Brauer et al., 1999, Lücke and Brauer, 2004). The onset of the Holocene is marked by the change in sedimentation from clastic-organic varves to predominantly organic varves (couplets, organic varve facies 1) separated by a short (4 cm) interval of poor varve preservation at the transition (756-750 cm; 11 640 - 11 590 varve a BP) (Fig. 3). Well preserved organic varve facies 1 is temporarily replaced by the organic varve facies 2 between 664-682 cm depth (10 530 and 9655 varve a BP), which is a 21 cm thick interval of organic rich sediment with occasional calcite layers and where detrital sublayers became thinner or are not present. We have labelled this episode as `black interval´ because of the dark appearance of the sediment core at this position (Figs. 2, 3), which makes varves undetectable by naked eye. Microscopically visible slump deposits (disturbed varves) appear in a 3 cm section at the bottom of this interval (682-679 cm), where 26 varves were interpolated (Figs. 2, 3b). At the top of the black interval (664 cm), a 1.5-cm-thick micro-disturbance followed by an abrupt facies-change indicates the presence of the hiatus mentioned above (Brauer et al., 2000; Fig. 3b).

[INSERT FIGURE 3 HERE]

Five intervals of thicker varves (mean thickness > 0.46 mm) have been identified: 11 590 – 11 540 varve a BP (0.95 mm), 11 230 – 11 165 varve a BP (0.7 mm) 10 690 – 10 610 varve a BP (0.77 mm), 9480 – 9340 varve (0.56 mm) and 9300 – 9035 varve a BP (0.54 mm). Discrete graded, reddish detrital layers occur more frequently just before the black interval at 10 650 varve a BP and in the sediment section deposited after 9655 varve a BP (Fig 3b).

4.3 μ-XRF core scanning

Intervals with similar geochemical compositions were established statistically using Ward's hierarchical clustering analysis of the clr-transformed μ-XRF data. Hierarchical clustering results are typically represented as a hierarchical dendrogram of minimum variance linking distances and assigning each individual data point to one of the statistical clusters (Fig. 4a). As such, showing clustering results stratigraphically down-core can be used to objectively identify different compositional intervals (Fig. 5g). A solution with 6 clusters was selected based on the relative linking distances (Fig. 4) together with the match between the cluster stratigraphy, core description and microfacies analyses (Fig. 5a). Statistical results are influenced by the number of data points in a cluster and tend to reflect more general compositional changes. Matching solutions with more than 6 clusters would exceed the variations acquired by core observations and microfacies analyses.

[INSERT FIGURE 4 HERE]

[INSERT FIGURE 5 HERE, Please place Fig. 4 and Fig. 5 next to each other]

The six clusters differentiate compositional changes based on the simultaneous variations of all elements acquired with μ-XRF core scanning.

These compositional changes are visualized using covariance biplots of the PCA loadings of the first two principal components (Fig. 4b). Positively correlated elements will have a similar orientation in the biplot, whereas negatively correlated elements are located opposite of each other. The six clusters reveal similar groups of elements (Fig. 4), which are indicative for detrital sediments (Ti, K and partly Si), diatom silica (Si), calcite (Ca), and redox sensitive elements (Mn and Fe). Iron is predominantly linked to the presence of vivianite, siderite and pyrite that form under reducing conditions (Brauer et al., 2000). Therefore, all clusters indicate that Fe is poorly or even negatively correlated with the detrital elements suggesting partly or completely diagenetic reduction of the original iron bearing minerals from volcanic country rocks, which allows the use of Fe as a redox proxy (Fig. 4b).

Cluster 1 (n=709) reveals a good correlation of the detrital elements and Si (Fig. 4b) indicating that diatom silica plays only a minor role in these sediments. The occurrence of cluster 1 in the stratigraphic sediment column coincides with high values of Ti_{clr}, thus representing minerogenic-rich sediments. In contrast, cluster 4 (n=1300), 5 (n=759) and 6 (n=159) agree in a clear negative correlation between the detrital elements and Si probably indicating distinct diatom bloom layers. Additionally, clusters 5 and 6 are influenced by calcium-bearing sediments, as indicated by increased ln(Ca/Ti) ratios (Fig. 5). In contrast, cluster 3 (n=1753) shows an influence solely of the Ca variability (Fig. 4) which, however, is not related to an increasing abundance of Ca as shown by low ln(Ca/Ti) ratios. The latter is further supported by microfacies analyses since no major contribution of calcium-rich minerals has been observed. Clusters 2 (n=368) and 3 show an intermediate situation where the detrital elements and Si are decoupled revealing a less clear division between the deposition of the detrital and diatom sub-layers, likely because of partly overlapping or mixed sub-layers. Regarding the redox sensitive elements, Fe and Mn are positively correlated in cluster 3, 5 and 6, while they are not correlated in cluster 1 and 4. The stratigraphical distribution of the major clusters allows to objectively distinguishes six geochemical boundaries at 11 555, 11 230, 10 650, 10 515 and 9670 varve a BP (Fig. 5g).

During the early Holocene until 5000 varve a BP the varve thickness is primarily controlled by the deposition of detrital sediments (thickness of the autumn/winter sub-layer) (Martin-Puertas et al., 2012b) except for the aforementioned ‘black interval’. Accordingly, relative variations of the varve thickness resemble the variability of Ti_{clr} (Fig. 5b, c), which is considered a proxy for minerogenic components because of the basaltic composition of the catchment (Martin-Puertas et al., 2012b). Variations of diatom abundances as inferred from microfacies analyses (spring/summer sub-layer) correspond well to variations of detrital-normalized silica represented by ln(Si/Ti) ratios (Martin-Puertas et al., 2012b). However, the detailed ln(Si/Ti) record suggests that diatom deposition has no substantial influence on the variations of the total varve thickness (Fig. 5b, d). The exceptional `black interval´ is characterised by lowest sedimentation rates, as well as very low contents of detrital matter as indicated by low Ti_{clr}, whereas higher ln(Si/Ti) and ln(Ca/Ti) ratios reveal an increase in relative concentrations of diatom silica and calcite, respectively (Fig. 5c, d, e). This supports thin-section observations of triplets of spring/summer diatom bloom followed by an endogenic calcite sub-layer and thin laminae of amorphous and particulate organic detritus (organic varve facies 2, Fig. 3c). An abrupt increase in the ln(Fe/Mn) ratio at 756 cm distinguishes YD sediments (low ratios) from Holocene-sediments (high ratios) (Fig. 5a, f).

5. Discussion

5.1. Depositional stages

High-resolution µ-XRF core scanning data in combination with microfacies analyses allow determination of changes in depositional environments in terms of sediment sources and sediment formation mechanisms. Hierarchical clustering of the µ-XRF core scanning data provides a tool to regard changes of a comprehensive set of elements simultaneously. This allows identification of compositional changes of elements that are not constrained to a single mineral phase. Consequently, we will use geochemically defined boundaries based on the clustering results and microfacies observations to discuss the major depositional stages in the MFM record (Fig. 5).

Depositional *stage I* (11 640 - 11 555 varve a BP) comprises the 4-cm interval of poor clastic varve preservation at the biostratigraphically defined YD-Holocene transition (Litt and Stebich, 1999; Brauer et al., 1999) and also includes the first 3 cm of Holocene organic varves (Fig. 5). This stage is characterised by cluster 2 (orange), which shows a decoupling of the Si from the detrital elements Ti and K (Fig. 4). This suggests a clear separation between the deposition of detrital material and a diatom layer, indicating the formation of seasonal couplets (although in parts poorly preserved) and hence supporting varve interpolation along the first 4 cm of the *stage I* (Fig. 2, Fig. 5b). Additionally, the boundary between *stages I* and *II* is marked by a sudden increase in the ln(Fe/Mn) ratios (Fig. 5g) reflecting a change to strengthened diagenetic processes and more anoxic bottom water conditions in the early Holocene. The sediments in this interval are further characterised by increasing organic contents.

Depositional stage *II* (11 590 to 11 230 varve a BP) is mainly represented by cluster 4 (light green) and followed by stage *III* (11 230 to 10 650 varve a BP) that is characterised by alternations of cluster 3 (dark green) and 4 (Fig. 5) and continuous sedimentation of organic varve facies 1 (couplets). The compositional differences of cluster 3 from cluster 4 are not easily detectable by microfacies observations. Cluster 3 corresponds to thicker varves with a predominant detrital sub-layer suggesting a higher detrital input (runoff) into the lake. The biplots also show different element correlations for clusters 3 and 4 (Fig 4b). The most distinct difference appears from the correlation between Si and detrital elements Ti and K, which is slightly positive for cluster 3 but negative for cluster 4. Also, the positive correlation of the redox sensitive elements Fe and Mn in cluster 3 is not apparent in cluster 4. These differences suggest a less strict separation of the siliciclastic and diatom sub-layers and stronger redox conditions in *stage III*, where cluster 3 is predominant. Changes in the separation between the siliciclastic and diatom sub-layers could be explained by changing seasonality since an additional late summer bloom partly overlaps with the autumn/winter layer composed of detrital and resuspended material. Diatom assemblages of the MFM sediments show high variability in both the genus of diatoms (species has not been specified) and the number of diatom blooms, *i.e.* varves with only one bloom of either *Stephanodiscus sp.* or *Cyclotella sp*, and varves with two blooms (*Stephanodiscus sp.* and *Cyclotella sp*) (Martin-Puertas et al., 2012b). Alternatively, the less strict separation between siliciclastic and diatom sub-layers might also be caused by resuspension of sediments from the littoral zone comprising epiphytic diatoms during autumn as observed by microfacies analyses. The interpretation of the loading of Ca in cluster 3 (Fig. 4) remains elusive because calcium-bearing minerals are too sparse to be detected even by microscopic analyses. This is supported by absence of significant occurrences of calcium-bearing minerals as derived from thin section analyses, which prevent us from a credible explanation for the Ca eigenvector in cluster 3.

The boundary between depositional stage *III* and stage *IVa* occurred at 10 650 varve a BP. Stage *IVa* is characterised by the deposition of four thicker (1-3 mm) discrete graded detrital layers (Fig. 3b) intercalated within the organic varve facies 1 and dominated by clusters 3 and 4 (Fig. 5). The detrital layers occurring in depositional stage *IVa* coincide with cluster 1 (yellow, Fig. 5g), which is characterized by the positive correlation of Si and the detrital elements Ti and K (Fig. 4b) demonstrating the siliciclastic nature of these event layers. A such, sediments related to cluster 1 and identified as discrete graded detrital layers are interpreted as surface runoff events. Most likely, these events are triggered by heavy rainfall and/or flood events and occur more often after 10 650 varve a BP.

Depositional stage *IVb* (10 515 to 9670 varve a BP) reflects the \`black interval´ (Fig. 5). As mentioned above, this episode is easily recognisable in the sediment sequence, even by naked eye. The boundaries at the bottom and the top are characterised by ~20 disturbed varves each, with an assumed hiatus of 240 years at the top (Brauer et al., 2000). Varve deformations show a fold structure suggesting micro slumps that caused the hiatus at the end of the stage *IVb* (Fig. 3b). Clusters 5 and 6 (light and dark blue) represent the sediments deposited during the stage *IVb* (Fig. 5g and 5), which differ considerably from the other early Holocene sediments. The most significant features of this stage are the strongly reduced detrital supply to the lake (low values of Ti_{clr}; Fig. 5b, c) resulting in very low mean varve thickness of 0.2 mm, as well as the formation of annual triplets (organic varve facies 2). The biplots corresponding to clusters 5 and 6 reveal a negative correlation of the Ti and Si (Fig. 4) that is most likely due to the occurrence of seasonal diatom blooms. Also, both clusters show that Ca is decoupled from the detrital elements Ti and K suggesting that Ca reflects endogenic calcite (Fig. 4). Difference between cluster 6 and 5 may corresponds to higher values of the ln(Ca/Ti) ratio and thicker calcite layers in cluster 6, while cluster 5 represents sediments with lower Ca values and thinner calcite varves during the *stage IVb* (Fig. 5). Calcite varves are exceptional in the MFM sediments and only occur within the *stage IVb* and a short interval in the Allerød (Engels et al., 2016). Calcite precipitation in mid-latitude lakes is mainly induced by either seasonal increase in the photosynthetic uptake of CO_2 and/or periodic calcite supersaturation due to increasing water temperature following the spring mixing (Kelts and Hsü, 1978). Primary productivity during the *stage IVb*, however, is not as strong as during other intervals where calcite did not precipitate, *e.g.* during the 2.8 ka climatic oscillation (Martin-Puertas et al., 2012a). Therefore, an alternative explanation for the formation and preservation of calcite varves in this interval might be an increased flux of

Ca^{2+} ions through groundwater input. Periods of elevated groundwater discharges into MFM have been reported during the early Holocene (Schettler et al., 1999). The most significant and prolonged peak in groundwater discharge (D2 in Schettler et al., 1999) coincides well with our stage *IVb*, which supports our interpretation (Fig. S1).

The stage *IVb* represents a unique episode in the history of the lake MFM intercalated within the continuous deposition of organic varve facies 1 (couplets), which characterises the entire MFM sediment record during the entire Holocene (Brauer et al., 2000; Martin-Puertas et al., 2012b). Following this depositional stage, the sediments are again characterised by organic varve facies 1 and episodic flood events (stage *IVc*), which coincide with clusters 3 and 1 respectively (Fig. 5).

5.2. Sediment responses to catchment evolution and climatic change

In order to evaluate the possible influence of the catchment and/or climate on the evolution of the lake, the geochemically-defined stages and Ti_{clr} (runoff proxy) are compared to i) the early Holocene pollen record from MFM, as an indicator of vegetation cover and catchment stability; and ii) to the temperature-sensitive $\delta^{18}O_{ice}$ Greenland ice core record (Rasmussen et al., 2006), as sensitive recorder of climatic oscillations in the North Atlantic region (Fig. 6).

[INSERT FIGURE 6 HERE]

The MFM pollen record reflects the major biostratigraphic boundaries defined in northern and central Europe, *i.e*, the YD/Holocene transition and the Preboreal/Boreal transition (Litt and Stebich, 1999). The non-varved interval included in the depositional stage *I* coincides with a peak in *Juniperus* pollen, indicating climatic amelioration already during the final stage of the YD (Brauer et al., 1999). Varves deposited before the stage *I* (mainly YD sediments) have graded silt layers at their base and are been interpreted as snowmelt deposits (Brauer et al., 1999). The Pleistocene-Holocene boundary as defined in the North-GRIP ice core (Walker et al., 2009) (Fig. 6) falls within our stage *I* within dating uncertainties. The onset of the Holocene as defined by biostratigraphy in MFM marks the rapid reforestation with the Preboreal-birch forest (*Betula*) (Litt and Stebich, 1999) and coincides with the end of the non-varved interval within the stage *I*. The sediment composition apparently responds with a short delay of a few decades compared to the vegetation change since stage *I* lasts until 11 555 varve a BP and include the first 3 cm of ca 35 organic-clastic varves after the biostratigraphic transition. That difference in the abruptness of the response of the sediment facies could be likely explained by the time until the vegetation was dense enough to reduce surface runoff and detrital material flux.

The Preboreal/Boreal transition is marked by a pronounced *Corylus* expansion, which reaches the maximum peak of >80% in the pollen diagram (Litt et al., 2009 at 10 700 - 10 650 varve a BP in the MFM region (Litt et al., 2009). Interestingly, the start of the *Corylus* increase coincides with the onset of the stage *IVa* at 10 650 varve a BP (Fig. 6) suggesting a close relation between vegetation cover in the catchment and sedimentation processes. Theuerkauf et al. (2014) suggest that the *Corylus* expansion in Europe was favoured by increasing wetness. This is supported by our data inferring the deposition of allochthonous runoff-triggered deposits within the stage *IVa, c* (cluster 1, yellow).

Unlike the depositional changes mentioned above, the boundaries that define the stage *IVb,* which occurred abruptly, do not have an equivalent signal in regional vegetation (Fig. 6). Local environmental thresholds, most likely related to hydrological conditions, are considered essential for these changes in the depositional system since the most significant features of the stage *IVb* is the lack of detrital (river) input and the formation of calcite varves (Fig. 5). Detrital supply into MFM predominantly originates from sediment discharge by the Meerbach stream that enters the crater in the south (Fig. 1). A possible explanation for the very low abundance of detrital matter in *stage IVb* is an increasing lake level causing flooding of the southern part of the crater that should have created a large shallow southern bay of the lake (Brauer et al., 1999). Such shallow bay (Fig. 1) should have acted as efficient trap for allochthonous detrital sediment influx. The strong decrease or even lack of detrital input to the deeper part of the lake suggests that flooding of the southern part of the crater probably reached a critical level between 10 530 and 9655 varve a BP. Rapid lake level increase at the onset and decease at the end of stage *IVb* even might have triggered the deposition of small-scale slump deposits in the deepest part of the lake since instable shorelines favoured avulsion from the littoral zone (Fig. 3b).

In contrast to the sedimentation changes related to vegetation during the early Holocene environmental amelioration, we do not find clear reflections of short-cold events identified in the Greenland ice cores at 11.4 ka b2k (PBO), 10.3 ka b2k and 9.3 ka b2k in the MFM sedimentary record (Fig.

6). The absence of sediment response, especially to the PBO, has been also reported from other lake sediments in northern and central-eastern Europe (Björck et al., 1997; Ott et al., 2016). One explanation for the absence of a sediment response in MFM to the PBO is that this fluctuation occurred during the strongest increase in tree pollen at the onset of the Holocene (Fig. 6), which might have superimposed environmental impacts of the climatic oscillation. The weaker climate oscillations at 10.3 and 9.3 ka b2k occurred during rather stable phases at MFM with dense *Corylus* cover in the catchment, which likely made the lake system resilient to these climate fluctuations.

6. Conclusions

We have demonstrated a multivariate statistical approach for the total µ-XRF core scanning dataset as a suitable tool to complement microfacies analyses and improve the interpretation of varved sediments. This approach allows linking compositional changes obtained by µ-XRF core scanning with micro-facies proxies to better identify mechanisms controlling the lake's depositional processes. In particular, our study on the MFM sediments confirms:

(1) The lake was sensitive to surface conditions in the catchment as controlled by long-term vegetation reorganisation and probably soil formation during the early Holocene.

(2) The lake sedimentation reacted abruptly to major biostratigraphic transitions in the early Holocene, i.e. the YD/Holocene and the Preboreal/Boreal transition.

(3) Hydrological thresholds promoted unprecedented conditions in the lake from 10 515 and 9670 varve a BP, characterised by a strong reduction of detrital supply to the deeper part of the lake and the precipitation of calcite.

(4) We found no clear sediment responses to short-term early Holocene climatic oscillations because of either superimposed major changes in vegetation or stable catchment conditions.

Acknowledgments

This study was funded by the GFZ German Research Centre for Geosciences, Potsdam, Germany, and is a contribution to the Helmholtz-Association climate initiative REKLIM (Topic 8 ‘Rapid Climate Change from Proxy data’) and supported by infrastructure of the Terrestrial Environmental Observatories network (TERENO) financed by the Helmholtz Association. The authors thank Agathe Deriot and Nadine Walikewtz for their contribution to the varve counting, Gert Jan Weltje for the extensive discussion of multivariate analyses of µ-XRF scanning data, Georg Schettler for providing data shown in Figure S1, Andreas Hendrich for the graphical support, Dieter Berger and Gabi Arnold for technical support with thin section preparation, and Brian Brademann and the coring team for recovering excellent cores. We also thank the editor Professor Geoff Duller and two anonymous referees for valuable comments on the manuscript.

References

Aitchison J (1982) The Statistical Analysis of Compositional Data. *Journal of the Royal Statistical Society. Series B. Methodological* 44: 139–177.

Björck S, Rundgren M, Ingólfsson O and Funder S (1997) The Preboreal oscillation around the Nordic \rSeas:terrestrial and lacustrune responses. *Journal of Quaternary Science* 12: 455–465.

Björck S. 2008: The late Quaternary development of the Baltic Sea basin. In Assessment of climate change for the Baltic Sea Basin, the BACC Author Team (eds). Springer-Verlag: Berlin Heidelberg; 398-407.

Bloemsma MR, Zabel M, Stuut JBW *et al.* 2012. Modelling the joint variability of grain size and chemical composition in sediments. *Sedimentary Geology* **280**: 135-148

Bos JAA, van Geel B, van der Plicht J and Bohncke SJP (2007) Preboreal climate oscillations in Europe: Wiggle-match dating and synthesis of Dutch high-resolution multi-proxy records. *Quaternary Science Reviews* 26: 1927–1950: doi:10.1016/j.quascirev.2006.09.012.

Brauer a, Endres C, Zolitschka B and Negendank JFW (2000) AMS radiocarbon and varve chronology from the annually laminated sediment record of Lake Meerfelder Maar, Germany. *Radiocarbon* 42: 355–368.

Brauer A, Endres C, Günter C, Litt T, Stebich M and Negendank JFW (1999) High resolution sediment and vegetation responses to Younger Dryas climate change in varved lake sediments from Meerfelder Maar, Germany. *Quaternary Science Reviews* 18: 321–329: doi:10.1016/S0277-3791(98)00084-5.

Czymzik M, Brauer A, Dulski D *et al.* 2013. Orbital and solar forcing of shifts in Mid- to Late Holocene flood intensity from varved sediments of pre-alpine Lake Ammersee (southern Germany). *Quaternary Science Reviews* **61**: 96-

110 [doi: 10.1016/j.quascirev.2012.11.010]

Dulski P, Brauer A, Mangili C. 2015. Combined μ-XRF and microfacies techniques for lake sediment analysis. In Developments in Paleoenvironmetal Research, Micro-XRF Studies of Sediment Cores, Applications of a Non-destructive Tool for the Environmental Sciences, Croudace IW, Rothwell RG (eds). Springer: Dordrecht, Netherlands; 325–349.

Engel S, Brauer A, Buddelmeijer N, Martin-Puertas C, Rach O, Sachse D, van Geel B (2016) Subdecadal-scale vegetation response to a previously unkown late-Allerød climate fluctuation and Younge Dryas cooling at Lake Meerfelder Maar (Germany). Journal of Quaternary Science 31: 741-752.

Grafenstein U Von, Erlenkeuser H, Brauer A, Jouzel J, Johnsen SJ and von Grafenstein U (1999) A Mid-European Decadal Isotope-Climate Record from 15 , 500 to 5000 Years B .P. *Science* 1654: 1654–1657: doi:10.1126/science.284.5420.1654.

Kelts K, Hsü K. 1978. Freshwater carbonate sedimentation. In: Lakes: Physics, Chemistry and Geology, Lerman A (ed). Springer: New York; 295–323.

Lauterbach S, Brauer A, Andersen N, Danielopol DI, Dulski P, Hüls M, et al. (2011) Multi-proxy evidence for early to mid-Holocene environmental and climatic changes in northeastern Poland. *Boreas* 40: 57–72: doi:10.1111/j.1502-3885.2010.00159.x.

Litt T, Stebich M. 1999. Bio- and chronostratigraphy of the lateglacial in the Eifel region, Germany. *Quaternary International* **61**: 5-16 [doi:10.1016/S1040-6182(99)00013-0]

Litt T, Schölzel C, Kühl N and Brauer A (2009) Vegetation and climate history in the Westeifel Volcanic Field (Germany) during the past 11 000 years based on annually laminated lacustrine maar sediments. *Boreas* 38: 679–690: doi:10.1111/j.1502-3885.2009.00096.x.

Lücke A, Brauer A. 2004. Biogeochemical and micro-facial ngerprints of ecosystem response to rapid Late Glacial climatic changes in varved sediments of Meerfelder Maar (Germany). *Palaeo- geography, Palaeoclimatology, Palaeoecology* **211:***139-155*.

Martin-Puertas C, Matthes K, Brauer A, Muscheler R, Hansen F, Petrick C, et al. (2012a) Regional atmospheric circulation shifts induced by a grand solar minimum. *Nature Geoscience* 5: 397–401. doi:10.1038/ngeo1460.

Martín-Puertas C, Brauer A, Dulski P and Brademann B (2012b) Testing climate-proxy stationarity throughout the Holocene: An example from the varved sediments of Lake Meerfelder Maar (Germany). *Quaternary Science Reviews*. Elsevier Ltd 58: 56–65. doi:10.1016/j.quascirev.2012.10.023.

Masson-Delmotte V, Landais a., Stievenard M, Cattani O, Falourd S, Jouzel J, et al. (2005) Holocene climatic changes in Greenland: Different deuterium excess signals at Greenland Ice Core Project (GRIP) and NorthGRIP. *Journal of Geophysical Research D: Atmospheres* 110: 1–13: doi:10.1029/2004JD005575.

McDermott F, Mattey DP and Hawkesworth C (2001) Centennial-scale Holocene climate variability revealed by a high-resolution speleothem delta 18O record from SW Ireland. *Science (New York, N.Y.)* 294: 1328–31: doi:10.1126/science.1063678.

Negendank JFW, Brauer A, Zolitschka B. 1990. Die Eifelmaare als erdgeschichtliche Fallen und Quellen zur Rekonstruktion des Paläoenvironments. *Mainzer geowissenschaftliche Mitteilungen* **19**: 235-65.

Ott F, Wulf S, Serb J, *et al.* 2016. Constraining the time span between the EarlyHolocene Hässeldalen and Askja-S Tephras through varve counting in the Lake Czechowskie sediment record, Poland. *Journal of Quaternary Science* **31**: 103-113[doi: 10.1002/jqs.2844]

Rasmussen SO, Bigler M, Blockley SP *et al*. 2014. A stratigraphic framework for abrupt climatic changes during the Last Glacial period based on three synchronized Greenland ice-core records: refining and extending the INTIMATE event stratigraphy. *Quaternary Science Reviews* **106**: 14–28 [doi:10.1016/j.quascirev.2014.09.007].

Rasmussen SO, Andersen KK, Svensson AM, Steffensen JP, Vinther BM, Clausen HB, et al. (2006) A new Greenland ice core chronology for the last glacial termination. *Journal of Geophysical Research* 111: D06102: doi:10.1029/2005JD006079.

Rasmussen SO, Vinther BM, Clausen HB and Andersen KK (2007) Early Holocene climate oscillations recorded in three Greenland ice cores. 26: 1–14.

Renssen H (2001) The climate in the Netherlands during the Younger Dryas and Preboreal: Means and extremes obtained with an atmospheric general circulation model. *Geologie en Mijnbouw/Netherlands Journal of Geosciences* 80: 19–30.

Schettler G, Rein B, Negendank JFW. 1999. Geochemical evidence for Holocene palaeodischarge variations in lacustrine records from the Westeifel Volcanic Field, Germany: Schalkenmehrener Maar and Meerfelder Maar. *Holocene* **9**: 381-400.

Tallantire PA (2002) The early-Holocene spread of hazel (Corylus avellana L.) in Europe north and west of the Alps: an ecological hypothesis. *The Holocene* 12: 81–96: doi:10.1191/0959683602hl523rr.

Theuerkauf M, Bos J a a, Jahns S, Janke W, Kuparinen A, Stebich M, et al. (2014) Corylus expansion and persistent openness in the early Holocene vegetation of northern central Europe. *Quaternary Science Reviews*. Elsevier Ltd 90: 183–198. Available at: http://dx.doi.org/10.1016/j.quascirev.2014.03.002: doi:10.1016/j.quascirev.2014.03.002.

Tjallingii R, Röhl U, Kölling M and Bickert T (2007) Influence of the water content on X-ray fluorescence core-scanning measurements in soft marine sediments. *Geochemistry, Geophysics, Geosystems* 8: n/a-n/a. Available at: http://doi.wiley.com/10.1029/2006GC001393: doi:10.1029/2006GC001393.

Weltje GJ and Tjallingii R (2008) Calibration of XRF core scanners for quantitative geochemical logging of sediment cores: Theory and application. *Earth and Planetary Science Letters* 274: 423–438. Available at: http://linkinghub.elsevier.com/retrieve/pii/S0012821X08004974: doi:10.1016/j.epsl.2008.07.054.

Wohlfarth B, Lacourse T, Bennike O, Subetto D, Tarasov P, Demidov I, et al. (2007) Climatic and environmental changes in north-western Russia between

15,000 and 8000calyrBP: a review. *Quaternary Science Reviews* 26: 1871–1883: doi:10.1016/j.quascirev.2007.04.005.

Zolitschka B, Brauer a., Negendank JFW, Stockhausen H and Lang a. (2000) Annually dated late Weichselian continental paleoclimate record from the Eifel, Germany. *Geology* 28: 783–786: doi:10.1130/0091-7613(2000)28<783:ADLWCP>2.0.CO.

Walker M, Johnsen S, Rasmussen SO *et al.* (2009) Formal definition and dating of the GSSP (Global Stratotype Section and Point) for the base of the Holocene using the Greenland NGRIP ice core, and selected auxiliary records. *Journal of Quaternary Science* 24: 3-17.

Table 1. Description of the marker layer used to transfer the MFM2000 chronology (MFM-6) to the MFM-9 profile, where µ-XRF data were measured.

Marker layers	**Description**	**Scale of identification**	**Age (varve a BP)**	**MFM-6 Depth (cm)**	**MFM09 Depth (cm)**
KL8	Detrital layer	Macroscopic	9340	627.5	647
K632	Detrital layer	Microscopic	9432	632.5	652
K640	Detrital layer	Microscopic	9581	638	658
K644	Detrital layer	Microscopic	9677	644	663
K652	Thick organic layer	Microscopic	10 168	653.5	673
KL9	Detrital layer	Macroscopic	10 632	666	686
UMT	Tephra layer	Microscopic	11 000	691	711
K9	Detrital layer	Microscopic	11 223	701	721.5
15 A	Detrital layer	Microscopic	11 416	713	735.2
YD	Non-varved/varved sediment transition	Macroscopic	11 584	726	750.7

Figure 1. Maps and aerial photo of MFM indicating topography of the crater, the bathymetry of the lake and the locations of the coring sites (yellow circle).

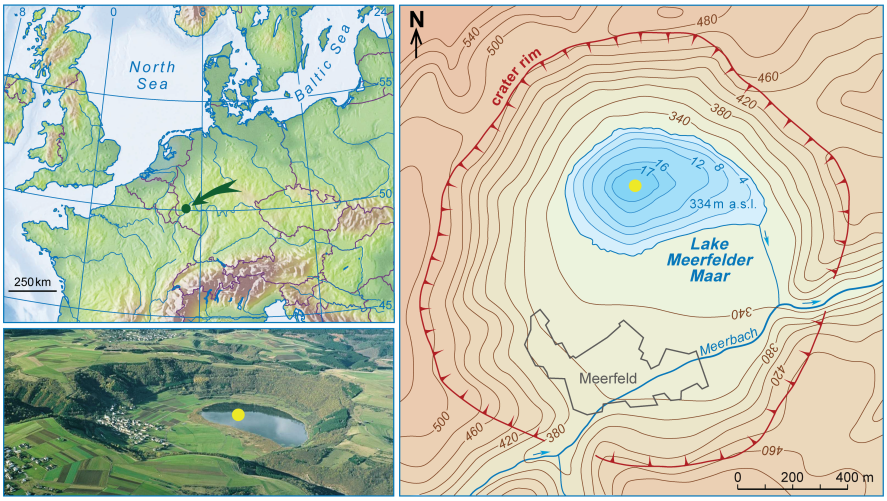

Figure 2. MFM-2012 chronology for the early Holocene sequence in Lake Meerfelder Maar. Age-depth model for both profile MFM09 and MFM-6, as well as marker layers used for correlation. Depth scale of the corresponding sediment sequence in MFM09 (left) and MFM-6 (right). Depths in all figures and main text refer to the MFM09 composite profile. Dashed lines indicate varve interpolation.

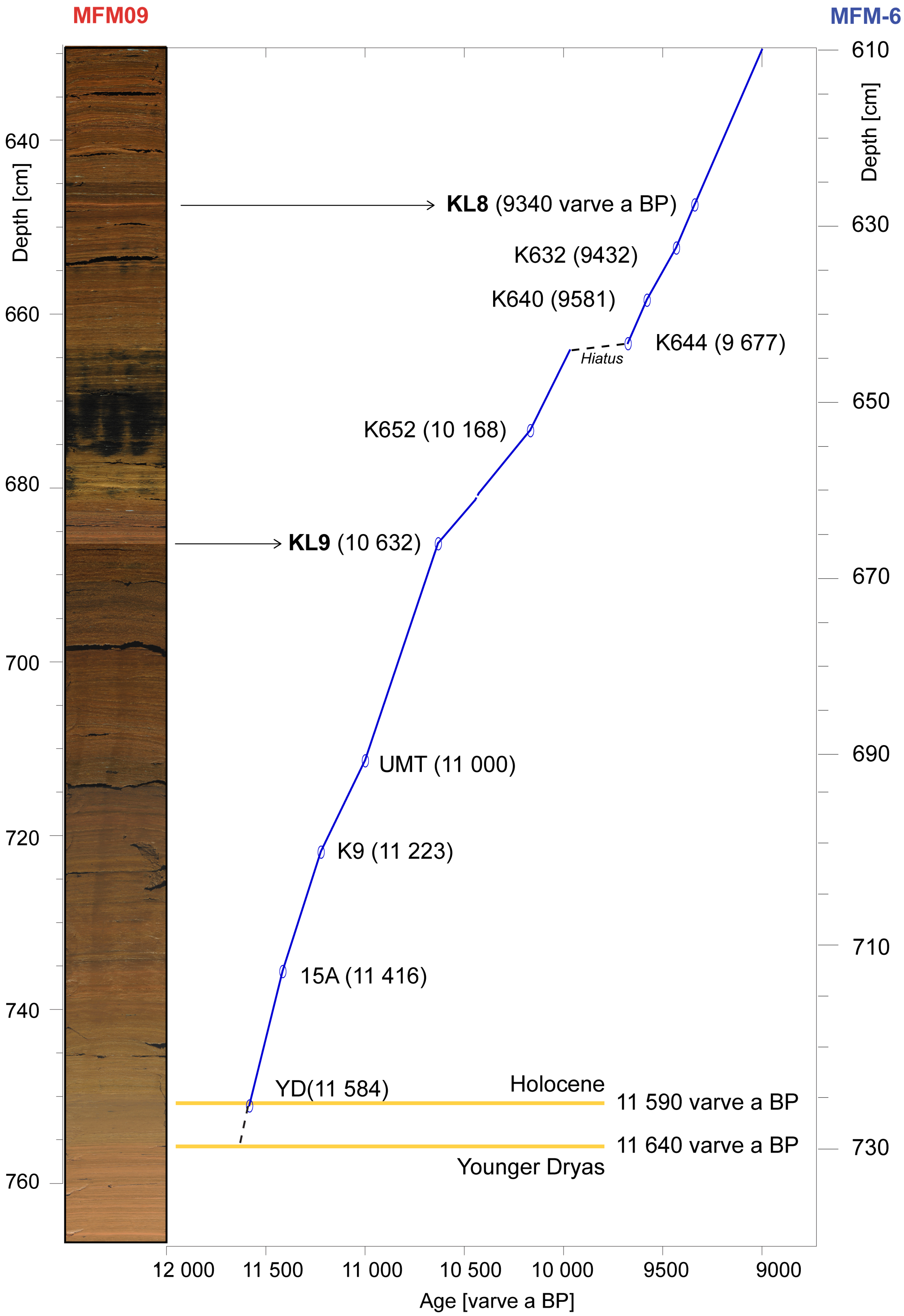

MFM09
MFM-6
Depth [cm]
640
660
680
700
720
740
760
610
630
650
670
690
710
730
KL8 (9340 varve a BP)
K632 (9432)
K640 (9581)
K644 (9 677)
Hiatus
K652 (10 168)
KL9 (10 632)
UMT (11 000)
K9 (11 223)
15A (11 416)
YD(11 584)
Holocene
11 590 varve a BP
11 640 varve a BP
Younger Dryas
12 000
11 500
11 000
10 500
10 000
9500
9000
Age [varve a BP]

Figure 3. Early Holocene sediment sequence of Lake Meerfelder Maar (MFM09). a) Core photo and lithological description; b) Microscopic polarised images of thin sections; c) Schema of the varve structure (seasonality) corresponding to the main varve facies described in the text.

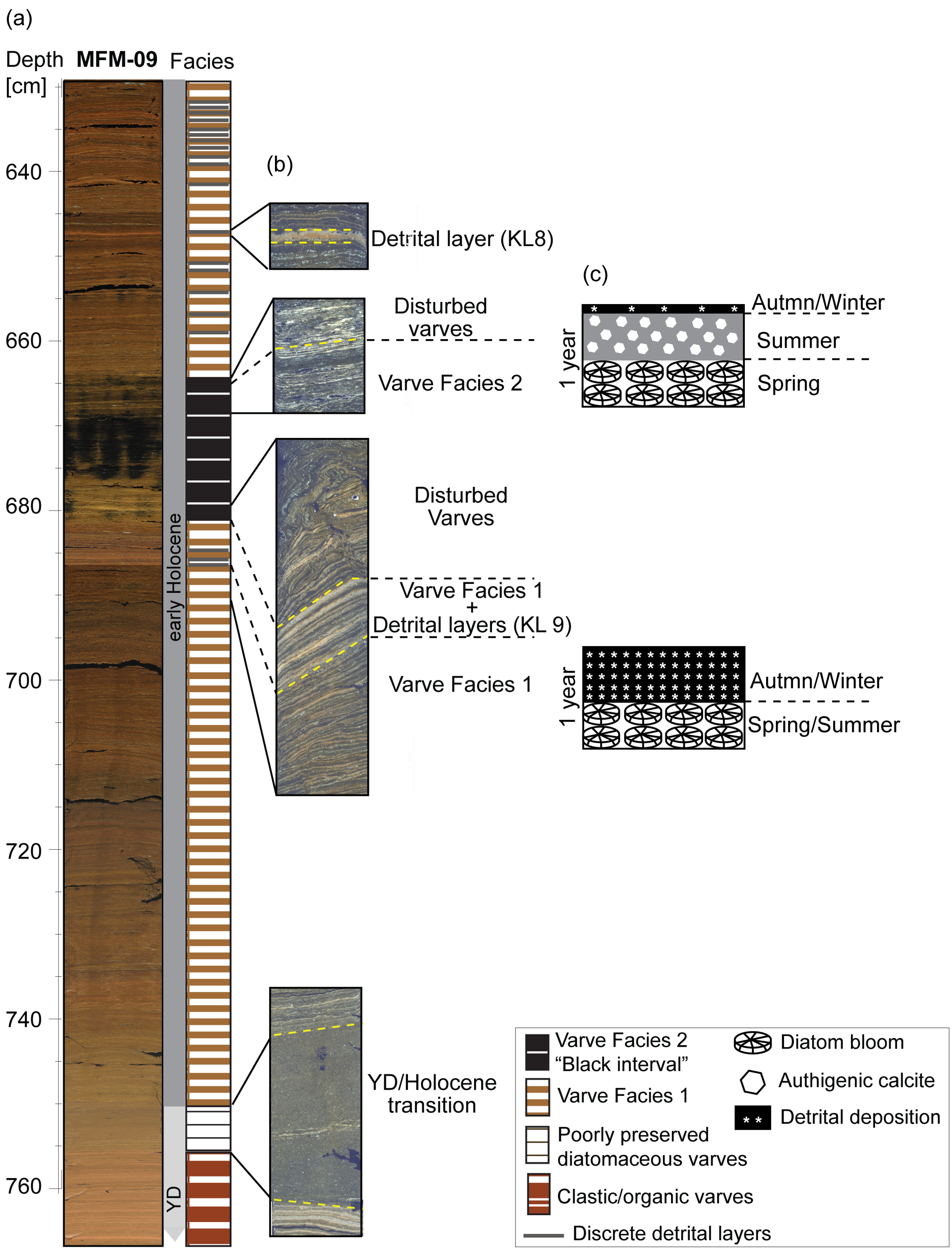

Figure 4. Hierarchical clustering results performed on the total µ-XRF core scanning data set. a) Clustering of the µ-XRF data provides objectively defined and statistical significant sub-composition of the sediments. b) Covariance biplot results of all individual clusters that visualize the correlation of main elements with respect to the first two principal components. The sub-compositions defined by 6-cluster solution matches with the sedimentological changes shown in Fig.5.

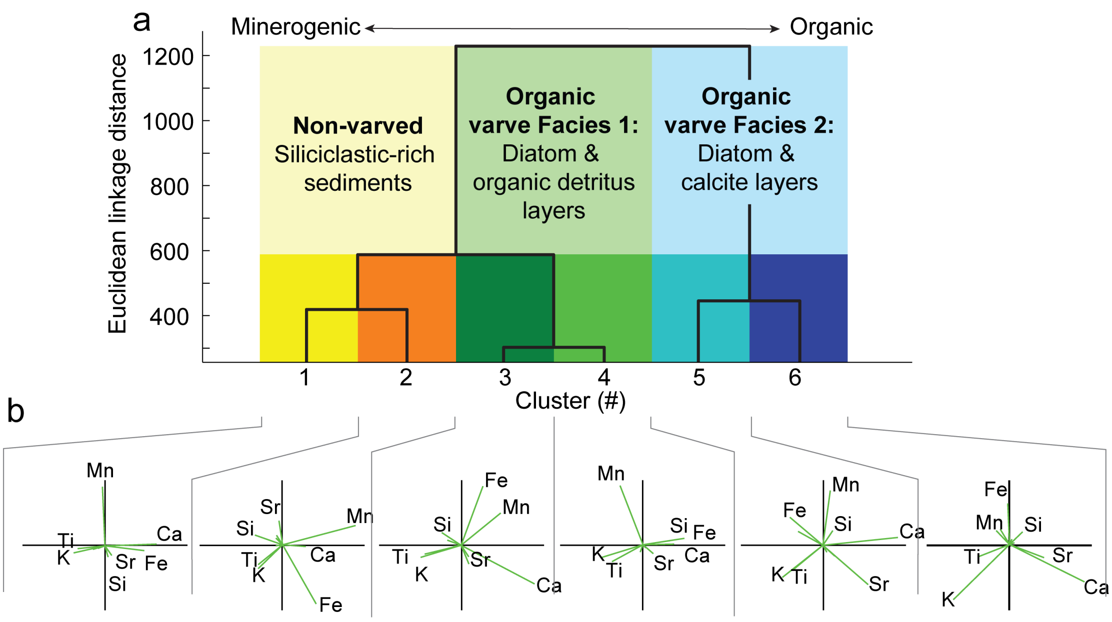

Figure 5. Environmental proxies from the early Holocene sediments of lake Meerfelder Maar. On depth scale a) core photo and lithology. On age scale b) varve thickness as a indicator for sedimentation rate mainly controlled by detrital input into the lake; c) centered-log ratio results of the Titanium (Ti_{clr}) as an indicator for relative changes of the bulk detrital matter; d-f) results of ln(Si/Ti), (Ca/Ti) and ln(Fe/Mn) indicating relative changes of biogenic silica concentrations, authigenic calcite precipitation and oxygenation at the bottom water, respectively; and g) Cluster stratigraphy with the down core

representation of the six clusters obtained from μ-XRF core scanning data and early Holocene depositional stages defined by the clustering results and microfacies observations.

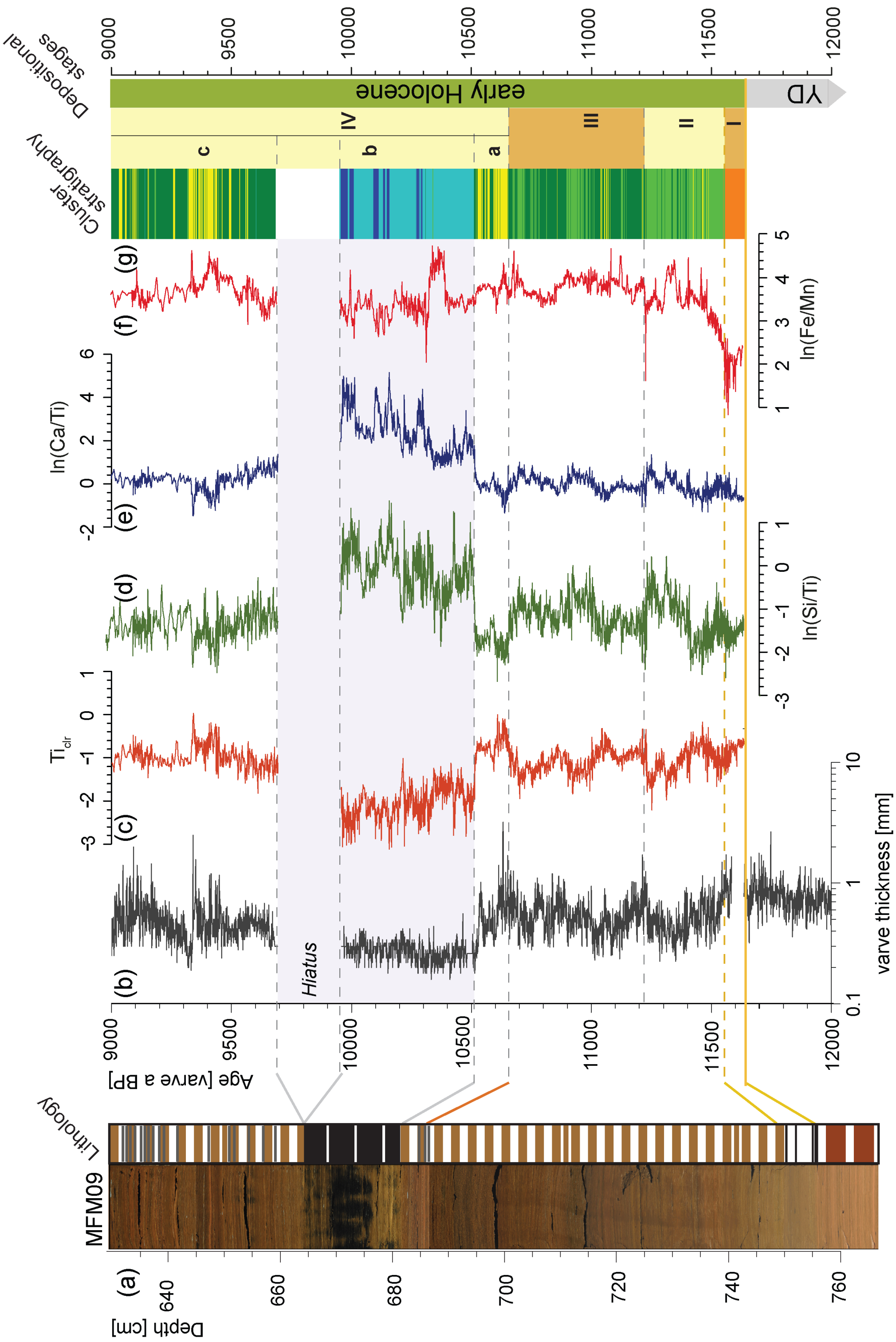

Figure 6. Regional comparison of high-resolution proxy records from Greenland and Meerfelder Maar during the Early Holocene. a) $d^{18}O_{ice}$ records from the Greenland ice cores GRIP and NorthGRIP both into the GICC05 timescale (Rasmussen et al., 2006, 2014); b-c) Pollen percentages from the MFM record (Litt et al., 2009); d) Stratigraphic representation of the six statistical clusters identified in the MFM sediments and depositional stages defined; e) Centered-log ratio results of the Titanium (Ti_{clr}, brown) and the 30-years running average (black) indicating relative changes of the bulk detrital matter.

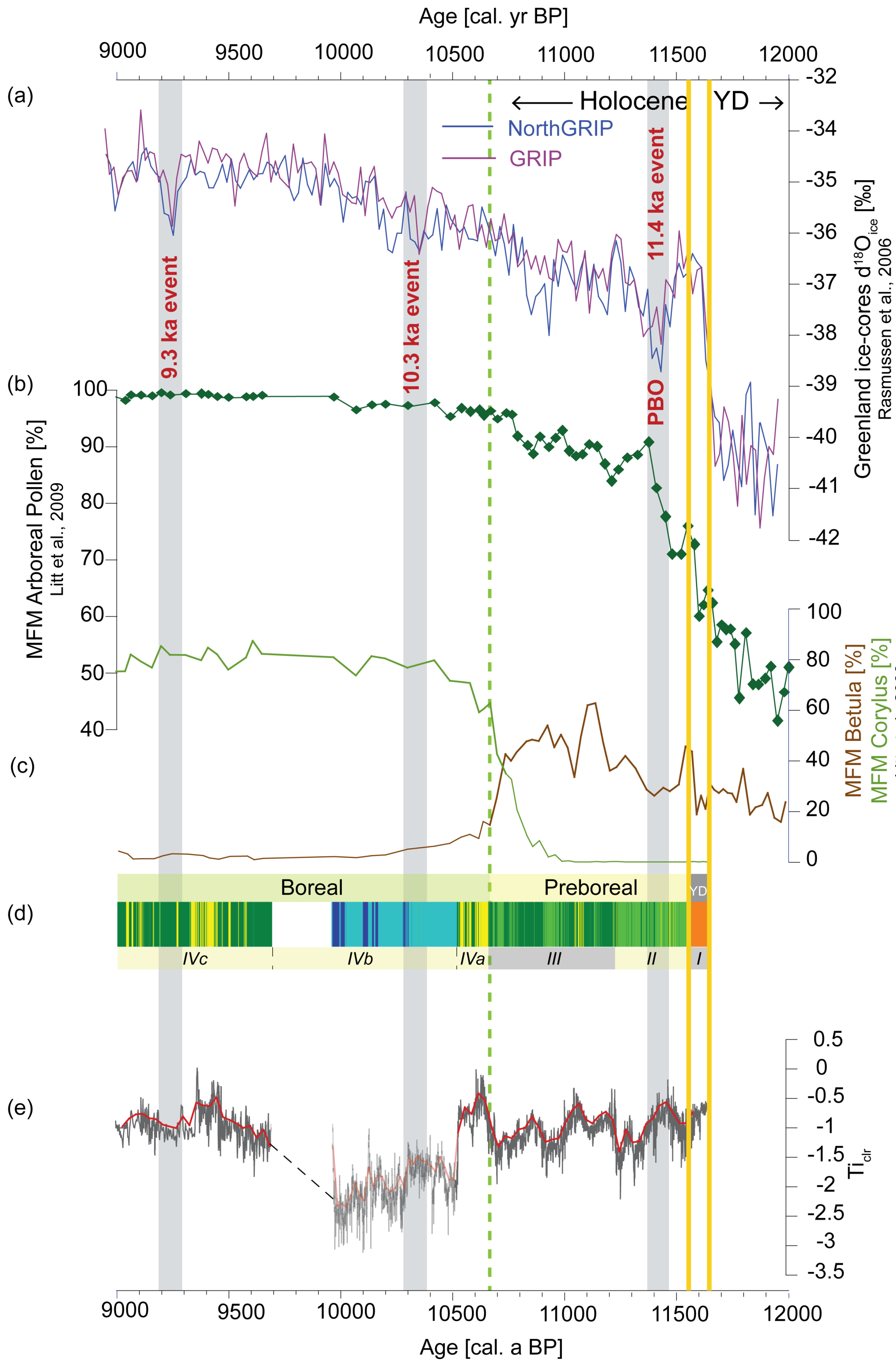
Age [cal. yr BP]
9000
9500
10000
10500
11000
11500
12000
(a)
← Holocene
YD →
NorthGRIP
GRIP
9.3 ka event
10.3 ka event
11.4 ka event
PBO
Greenland ice-cores d18Oice [‰]
Rasmussen et al., 2006
-32
-34
-35
-36
-37
-38
-39
-40
-41
-42
(b)
MFM Arboreal Pollen [%]
Litt et al., 2009
100
90
80
70
60
50
40
(c)
MFM Betula [%]
MFM Corylus [%]
Litt et al., 2009
100
80
60
40
20
0
(d)
Boreal
Preboreal
YD
IVc
IVb
IVa
III
II
I
(e)
Ticlr
0.5
0
-0.5
-1
-1.5
-2
-2.5
-3
-3.5
9000
9500
10000
10500
11000
11500
12000
Age [cal. a BP]

Figure S1. Groundwater discharges in the Lake Meerfelder Maar. Transference of the MFM2000 chronology to the composite profiles MFM 2a-2b (Schettler et al., 1999) via correlation with the percentage of total organic carbon (TOC). From bottom to top: U/Be ratio and percentage of TOC from the composite profile MFM 2a-2b published by Schettler et al (1999); percentage of TOC and age-depth model for the composite profile MFM-6. D1-D3 indicates positive groundwater discharge (Schettler et al., 1999). UMT: Ulmener Tephra Layer (11 000 varve a BP).